Наносистеми, наноматеріали, нанотехнології
Nanosistemi, Nanomateriali, Nanotehnologii
2022, т. 20, № 1, сс. 45–56

PACS numbers: 02.70.-c, 05.70.Ln, 61.48.De, 62.23.Hj, 62.25.Mn, 81.05.Lg, 83.10.Tv

Comparison of Strength and Competitiveness of Different-Length Carbon Fibres Equipped with Self-Healing Mechanism

V. I. Teslenko and O. L. Kapitanchuk

Bogolyubov Institute for Theoretical Physics, N.A.S. of Ukraine,
14b, Metrolohichna Str.,
UA-01143 Kyiv, Ukraine

Based on a three-stage kinetic model for description of deformation of a one-dimensional chain under tension in a plastic range, being applied to the decay of defects in a single carbon fibre within the one-defect approximation, the dependence of failure probability on tensile stress is obtained. A comparison of strength and competitiveness for the two different-length carbon fibres equipped with self-healing mechanism is carried out. Concerning with a numerical simulation of the theoretical failure distributions by the use of the accessible experimental data, it is shown that, in comparison with the longer carbon fibre, the shorter carbon fibre is advantageous in strength since the stress-distribution curve for the latter is on the right side, and that for the former is on the left side. On the other hand, the former distribution looks like a bimodal one and appears to be noticeably flatter than the latter distribution, which seems to be unimodal. This means that the longer carbon fibre is more advantageous in competitiveness than the shorter carbon fibre. It is concluded that, compared to the latter, the former may tolerate the greater change in the fracture stresses near the inflection point of the sigmoid distribution curve by keeping a higher load carrying capacity in a plastic range.

Ґрунтуючись на тристадійному кінетичному моделю для опису деформації одновимірного ланцюга під напруженням у пластичній області, застосованому до загасання дефектів у поодинокому вуглецевому волокні в однодефектному наближенні, одержано залежність ймовірности руйнувань від розтягувального напруження. Проведено порівняння міцности та конкурентоспроможности для двох різної довжини вуглецевих волокон, устаткованих механізмом самозагоювання. Піклуючись про використання експериментальних даних для проведення чисельної симуляції теоретичних розподілів руйнувань, показано, що довше вуглецеве волокно переважає у міцності коротше волокно, бо крива розподілу напруження для останнього знаходиться праворуч від першого. З іншого боку, перший розподіл виглядає бімодальним і виявляється

значно пологішим за останній, який виявляється унімодальним. Це означає, що довше вуглецеве волокно переважає коротше за конкурентоспроможністю. Зроблено висновок, що порівняно з останнім перше волокно у змозі витерплювати більшу зміну руйнувальних напружень, близьких до точки перегину кривої сигмоїдального розподілу, утримуючи вищу передану місткість навантаження в пластичній області.

Key words: self-healing systems, failure-prone states, defect decay, single carbon fibre, strength, competitiveness.

Ключові слова: самозагоювані системи, схильні до руйнування стани, загасання дефектів, поодиноке вуглецеве волокно, міцність, конкурентоспроможність.

(Received 12 April, 2021)

1. INTRODUCTION

Many material systems from designed glass–ceramic composites to advanced semiconductors are not perfect in structure but filled with defects of various types. These constantly occur within the systems in different numbers, which, when becoming too large, can be lowered below failure thresholds by using self-repairing and self-healing mechanisms. Preventing the onset of defects in flawless systems does not make sense for comparison of their competitive advantage over one another. Instead, defect-containing fallible systems do compete in strength and competitiveness and, therefore, are in need in comparison with each other [1, 2].

In competing systems, the source of their competitive advantage in achieving maximum quality performance is of basic interest. If system quality is associated with performance measured by productivity, the main source of competitive advantage is controllability of the rate ordered to populating a safe functioning state of the product manufacturing system [3]. In this case, the less the share of source resource providing a change in population is, the more controllable and hence performable system is. But, if the system quality is associated with tolerability of the failure-prone functional states with respect to defects, reliability and maintainability attributes typical of dependable manufacturing systems come into play [4].

In this case, instead, the more the share of source resource providing a change in population is, the more tolerable and hence competitive system is. There are also other sources of system competitive advantage such as relative size of shared state space, preferential attachment, quality durability, *etc.* [5, 6]. However, cardinality of the state space of the system depends exponentially on the number of its states. In the first case, these states are the right (or

safe functioning) states, while in the second case, they are the defect (or failed) states. However, quantifying competitiveness of systems requires consideration of their one-particle states in the mean-field approximation, with making the number of states as small as possible in both cases [7]. This allows quantifying a quality performance of the system in comparison with other systems of the same cardinality, based on the information only about their interstate transition probabilities [8, 9].

As the competitive advantage of the system treated in its defect state space is associated with the share of resource to provide a tolerable change in population of defect state appeared as weakest in respect to failure, the system competitiveness can similarly be assigned to a slope of response curve of the maximum of population of weakest defect state to a change in log failure rate. Thus, the system with lower sensitivity of that maximum will be superior in competitiveness compared to the system with higher sensitivity [10]. To describe transition probabilities between the states and derive the master equation for evolution of populations in a defect-state framework, we may use a perturbative treatment for the disordered solid as a nonequilibrium system weakly coupled to an equilibrium environment [11].

In this framework, the defect states are associated with the atomic configurations of a disordered phase of a solid, between which some atoms or groups of atoms move by random jumps from site to site through the solid [12, 13]. The interaction needed for the defect movement is treated microscopically as an effective coupling induced by phonon exchange between a disordered solid and its environment in the second order of perturbation theory and with using the polaron transformation [14]. This allows us to describe the temporal behaviour of a disordered solid, if the probabilities of transitions between its defect states are properly defined, and a comparison of theoretical predictions on fallible behaviour with experimental data on destructive testing is made.

There are a number of testing methodologies dependent on the type of the test method and a kind of detected defect [15–17]. For example, most detecting and correcting tests are non-destructive, whereas all mechanical tests are destructive [18]. Especially, the latter are ordered to obtain the cumulative distribution of probability of failure of the tested material by associating its different samples with some *ad hoc* systems and then counting a number of their failures at the different stresses. Examples of *ad hoc* systems running without interruption during a single testing event are numerous, from industrial and engineering systems [19] to polymers [20] and ceramics [21], and other brittle materials [22]. Furthermore, in order to be ready for the test, these systems must be

equipped with self-healing ability applied in many areas such as civil engineering, aerospace, common computer networks and intelligent systems of systems [23–27]. However, despite ubiquity in applications, there is a lack of theoretical models providing a unified description of strength and competitiveness of those systems based on the particular-use cases.

In the present paper, we address the above challenge by using the three-stage kinetic framework for evolution of decaying defects in a single carbon fibre within the one-defect approximation. That framework is regarded as a mesoscopic model for an *ad hoc* self-healing system having a single failure-prone state such that, when affected by the defect, is failed with non-zero probability, thus, leading to irreversible damage of the system [10]. We describe this model in detail in Sec. 2. Further, in Sec. 3, a probability distribution of a system failure in the dependence on tensile stress is found. Then, in Sec. 4, experimental data accessible for the different-length carbon fibres are compared with obtained theoretical results, which, finally, are discussed and concluded.

2. MESOSCOPIC MODEL OF DEFECT EVOLUTION IN A SINGLE CARBON FIBRE

There exist three characteristic scales for description of evolution of defects in different systems. These are microscale, mesoscale and macroscale. At the microscale, the defects are related to the excited states of a nonequilibrium quantum system weakly coupled to an environment [14]. It is assumed, despite different types of defects may occur in a system in all possible occupation numbers, there is the mean-field approximation that replaces an actual surrounding of the defect by a locally averaged number of neighbouring defects such that a single defect of most significant type will influence only one set of measurements [10]. Consequently, the many-defect state is specified in terms of occupation numbers (defect state populations) associated with the small elementary cells in the system in the single-defect state space. Remarkably, the kinetic equation for the state populations, being the result of averaging of the Liouville–von Neumann evolution equation for the density matrix of the whole system ‘a system + an environment + their weak interaction’ over fast fluctuations in the energy levels of defect states, is reduced to a population balance equation. An example of derivation of this equation with its application to a three-stage absorbing Markov chain within the one-defect approximation has been given in [10].

At the macroscale, the defects are related to macroscopic particles such as atomic or molecular species, whose concentrations vary with time and behaviour obeys the generalized continuity equation.

However, in the low-concentration limit and in the activated-state representation for single-defect structures, the equation of diffusion of defects can be reduced to the master equation for their thermally activated Arrhenius-type transitions between the failure-tolerant and the failure-prone defect states of the system [9, 11].

While microscale and macroscale defect descriptions are rather general, the mesoscale defect model presented in this section is more specific and gives a pictured description of the temporal behaviour of the material system in terms of its plastic-like distortions. Of course, that description is simplistic, but provides a simple dependence of the defect concentration on applied stress in the low-concentration limit.

Let us restrict ourselves to the mesoscale modelling of distortions in a single carbon fibre due to vacancy defects of plastic deformation appeared under tensile stress load. Consider a linear one-dimensional chain consisted of M identical units interacting through plastic-deformation fields characterized by the occurrence of extremely weak bonds between the nearest neighbours. At the thermodynamic equilibrium of chain loading, the change in the energy ΔG_σ of the tensile stress σ is compensated by the entropy $m_\sigma k_B T \ln C_\sigma$ of $m_\sigma = 1, 2, \ldots, M-1$ noninteracting defects randomly distributed among chain units with concentration $C_\sigma = m_\sigma (M-1)^{-1} \equiv (\bar{M}_\sigma - 1)^{-1}$, where $\bar{M}_\sigma = M[C_\sigma (M-1) + 1]^{-1}$ is the reduced number of units per one defect, with k_B and T being the Boltzmann constant and absolute temperature, respectively. However, at clamping of the tensile stress, that equilibrium does not hold and should be changed for transformation to take place, as additional stages would be emerged in the chain temporal behaviour.

This is illustrated in Figs. 1, *a*–*c* (on the left side of Fig. 1) by relating the defects to: the sector-like cavities randomly formed under applied tensile stress σ between some chain units in starting state $|3>$ (Fig. 1, *a*); the rectangular cavity signifying a single intermediate failure-prone state $|2>$ (Fig. 1, *b*); and the inverted sector-like cavity designating a final irreversibly decaying self-healing state $|1>$ (Fig. 1, *c*). Therefore, to describe the chain nonequilibrium dynamics in terms of kinetic equations for reversible and irreversible transitions between three nonstationary occupancy configurations, we must first define the defect state space $\{|3>, |2>, |1>\}$ for these configurations, then determine the stress-independent intrinsic energy levels (or enthalpies) $E_{3,2,1}$ characteristic of them, with accounting for self-healing *ad hoc* properties of one-dimensional chain under modelling, and finally specify the rate constants u_σ, v, a, b, k for transitions between the defect states in a one-defect approximation for a chain with a single failure-prone state.

Note, in such a mesoscopic setting, the only parameter, which bears

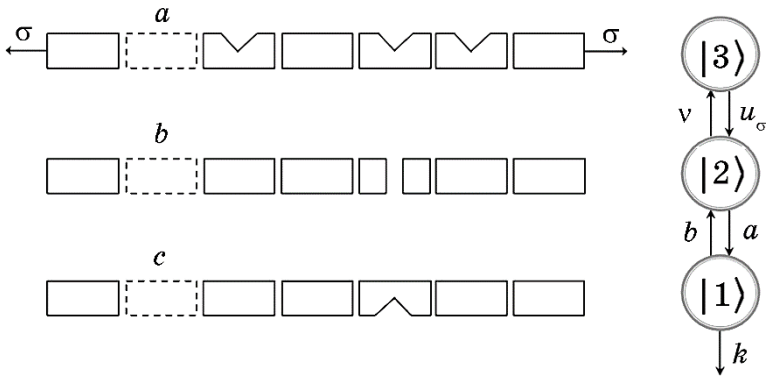

Fig. 1. Schematic for different configurations of one-dimensional chain with defects (sector-like or rectangular vacancies) under tensile stress σ in plastic range. Left: (*a*), (*b*) and (*c*) are initial failure-tolerant, transient failure-prone and pre-ultimate self-healing configurations, respectively. Right: kinetic scheme of states $|3>, |2>, |1>$ corresponding to configurations (*a*), (*b*), (*c*) with transition rate constants u_σ, υ, a, b, k (shown by arrows).

the dependence on the applied macroscopic stress σ, is the defect concentration C_σ in state $|3>$ directly related to the rate constant for transition of that state to state $|2>$ as $u_\sigma = u_\infty C_\sigma$, with u_∞ being a microscopic rate constant in the high-stress limit $\sigma \to \infty$ where the defect concentration in state $|3>$ reaches unity: $C_\infty = 1$. On the other hand, the defect concentration is exponentially dependent on tensile stress, corresponding to the reduced failure function as

$$C_\sigma = C_0 + 1 - \exp[-(\sigma - \sigma_0) / \sigma_9], \tag{1}$$

where C_0 and σ_0 are the shift and scale parameters chosen as some references. For instance, under plastic deformation, σ_0 is of the order of a few tens of MPa to be smaller than a representative yield strength, at which plastic deformation begins, and $C_0 > 0$ is the defect concentration at the stress $\sigma = \sigma_0$ that, in fact, does not start from the zero line but from a value of σ_0. Therefore, low stresses $\sigma \approx \sigma_0$ give a linear relation between stress and concentration, $(\sigma - \sigma_0) / \sigma_0 = C_\sigma - C_0$, analogous to the Hook's law, while high stresses $\sigma \gg \sigma_0$ lead to the damage of the system [28]. Hence, to characterize tensile stress experiments, we can use an approximate logarithmic relation model $\sigma = \sigma_0[1 - \ln(C_\sigma / C_0)]$ as a compromise between the two stress models, that is: a linear model $\sigma = \sigma_0 C_\sigma$ for relation of hydrostatic stress to concentration of atoms in a plate [29] with $C_0 = 0$ at low stresses, and a log–log model $\sigma = -\sigma_0 \ln\ln(C_\sigma)^{-1}$ for relation of tensile stress to defect concentration derived from (1) in the large-concentration limit $1 \geq C_\sigma \gg C_0 > 0$ at high stresses $\sigma \gg \sigma_0$. The latter model associated

with the link activation function [30] is widely used in various applications. For example, in neural networks and Markov chains, it indicates changes in the probabilities of states and the rates of transitions between states, which lead to the flattening of stress–strain plastic-deformation curves during strain hardening [31].

2. MASTER EQUATION AND CUMULATIVE DISTRIBUTION FUNCTION

The master equation for evolution of the nonnormalized state populations $P_{3,2,1}(t)$ is represented by the set of three kinetic equations as follows:

$$\begin{cases} \dot{P}_3(t) = vP_2(t) - u_\sigma P_3(t); \\ \dot{P}_2(t) = bP_1(t) - (v + a)P_2(t) + u_\sigma P_3(t); \\ \dot{P}_1(t) = -(b + k)P_1(t) + aP_2(t). \end{cases} \tag{2}$$

For the initial conditions,

$$P_3(0) = 1,\ P_2(0) = P_1(0) = 0, \tag{3}$$

typical for tensile testing materials [17, 32], solution of (2) for the population $P_2(t)$ of a failure-prone state $|2>$ in Fig. 1, *b* reads

$$P_2(t) = u_\sigma \sum_l \frac{b + k - \lambda_l}{\prod_{l' \neq l} (\lambda_l - \lambda_{l'})} \exp(-\lambda_l t). \tag{4}$$

Here, the exponents $\lambda_{l,l'=1,2,3}$ are system eigenvalues, which correspond to the nonnegative Debye relaxation rates obeying the characteristic equation [10]:

$$\lambda^3 - \lambda^2(u_\sigma + v + a + b + k) + \lambda[(u_\sigma + v)(b + k) + a(u_\sigma + k)] - u_\sigma ak = 0. \tag{5}$$

Thus, the temporal behaviour of $P_2(t)$ (4) represents an exponential rise and decay composed of three relaxation modes. Every mode adds the particular contribution differing in its eigenvalue, amplitude and sign. In general, the time dependence of (4) shows an increase, peak and decline without oscillations. So, we can determine for $P_2(t)$ the maximum

$$\bar{P}_2 = P_2(t_2^{peak}) \tag{6}$$

found at the peak time $t = t_2^{peak}$ as a nontrivial solution of the transcendent equation

$$\dot{P}_2(t) = 0\,, \tag{7}$$

and, then, associate such a maximum with the failure distribution of one-dimensional self-healing chain in the worst case.

Consequently, given the proportionality of the failure rate constant to the defect concentration, $u_\sigma = u_\infty C_\sigma$, and a simplified relation between log of the latter and the reduced applied stress in the form $\sigma / \sigma_0 = 1 - \ln(C_\sigma / C_0)$ obtained in the previous section, we can calculate from (4)–(7) the stress-dependence of cumulative distribution function

$$\bar{P}_2^{[\sigma]} = \bar{P}_2[\ln(u_\sigma / u_0)] \tag{8}$$

in its functional dependence on the reduced logarithmic failure-rate constant, which depends on the stress as

$$\begin{gathered} \ln(u_\sigma / u_0) \equiv \ln(u_\sigma / u_{0.5}) - \ln(u_0 / u_{0.5}) = -(\sigma - \sigma_0) / \sigma_0; \\ u_0 \equiv u_{\sigma_0} \ll u_\infty \equiv u_{\sigma\to\infty};\ \sigma \geq \sigma_0. \end{gathered} \tag{9}$$

So, we can compare either the cumulative distribution function (8) or the correspondingly scaled and shifted failure-distribution function,

$$\hat{P}_2^{[\sigma]} = \hat{P}_2[\log(u_\sigma / u_{0.5})]\,, \tag{10}$$

with the experimental data on tensile-stress testing of a single carbon material, where $u_{0.5}$ is an auxiliary rate constant, which depends on the material (for instance, its length) meaning a half point of failure-rate constant on sigmoid distribution curve (10). Fortunately, the quantity $\ln(u_0 / u_{0.5})$ in (9) does not depend on the sort of the material and may be accounted as the shift along the abscissa axis with a constant parameter $2.303\sigma_0$, where 2.303 is the logarithmic conversion factor from log to ln. On the contrary, the value of $u_{0.5}$ depends on the material and must be taken into account as an adjusted parameter for purposes of comparison with experiment from the very beginning.

3. COMPARISON OF EXPERIMENTAL DATA TO OBTAINED THEORETICAL RESULTS WITH DISCUSSION AND CONCLUSIONS

In the previous sections, we propose a three-stage kinetic model for defect dynamics under the tensile stress in plastic range of one-dimensional self-healing chain (see Fig. 1). To compare the obtained theoretical cumulative distribution (8) with the existing experimental data on the failure probability, we let the chain to be al-

lowed to adopt only a single stress test by presenting itself as a brittle material with no significant plastic deformation before damage. At the same time, the chain is regarded as self-healing. Therefore, it is not necessarily failed even when applied stress achieves a particular threshold, but, according to self-healing ability, can tolerate any finite stress without failure with nonzero probability. Just such behaviour is seen in the composite material case, for example, a ductile matrix reinforced by a brittle carbon fibre. Remarkably, the latter is fabricated in various length scales and diameters, ranging from macroscale (as-received woven fabrics) to mesoscale (fibre tow diameter) to microscale (a single fibre diameter) and nanoscale (nanofibre diameter) [32, 33]. Moreover, the carbon fibre is generally characterized by the self-organizing capability of the aromatic carbon to orient graphite crystallites, either spontaneously or by heat treatment, along the fibre axis in the relaxed state [34]. Such a fibre is subjected to the number of intrinsic defects associated, for example, with dislocations, disordered interfibrillar carbon, misoriented crystallites and other fracture-initiating flaws of unknown kind [35]. Hence, it is natural to regard that to be the strong, perfectly elastic material at the low stress in elastic range, but only an occasionally (with a nonzero probability) brittle material at the higher stress in plastic range, a single carbon fibre must be equipped with its own self-healing mechanism manifested itself as, for instance, an irreversible decay stage in the multistage defect dynamics model (cf. Fig. 1).

Thus, leaving aside the problem on how defect can emerge in a single carbon fibre within the one-defect approximation and using a formal three-stage kinetic model for defect decay given in Fig. 1, we conclude this paper with results of comparing cumulative failure distribution (8) of that model with experimental data obtained in [36] from load-deflection curves for the two different-length carbon fibres. As seen in Fig. 2 displayed for long and short carbon fibres, respectively, the associated distribution plots appear to be essentially bimodal. Inspection of a sigmoid distribution fit to the corresponding data points in Fig. 2 and Table 1 is summarized in the following conclusions.

First, the use of *ad hoc* adjustable parameters for the rate constants $u_{0.5}$, v, a, b, k provides a good agreement between the theory and the experiment with a concern on revealing bimodal character of sigmoid cumulative distributions not falling into a family of the Weibull distributions [10]. This indicates the utility of a three-stage model in Fig. 1 to explain bimodality of failure distributions of carbon fibres by virtue of self-healing mechanism favouring the defect decay in plastic range.

Second, for longer and shorter carbon fibres, the corresponding parameters v, a, b, k are more close to each other than a parameter $u_{0.5}$,

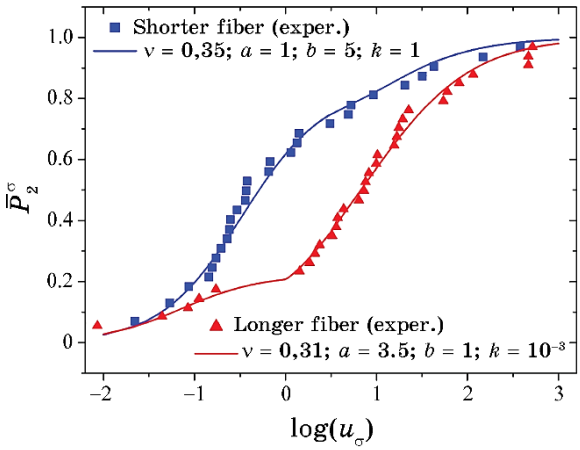

Fig. 2. Theoretical cumulative probability distributions of failures (curves (8) with parameters shown in insets) in comparison with experimental data (adapted from [37]) for longer (right) and shorter (left) single carbon fibres.

which is, accordingly, very distinct (see Table). This can be well understandable by revealing the fact that shorter carbon chain is generally stronger with higher strength than longer chain lower in strength.

Third, the sigmoid failure distribution for longer carbon fibre (left curve in Fig. 2) is flatter than that of shorter fibre (right curve in Fig. 2). This means that, for the longer (L) and the shorter (S) carbon fibres, the former tolerates greater change ratios of corresponding failure rate constants $u_{0.9}^{(L,S)}$ and $u_{0.1}^{(L,S)}$ at, say, 0.9 and 0.1 of sigmoid curve, respectively, by keeping the higher load carrying capacity given by the change in log failure rates as $\theta_{0.9-0.1}^{(L,S)} = \log[u_{0.9}^{(L,S)} / u_{0.1}^{(L,S)}]$ than the latter. From Table, we see that $\theta_{0.9-0.1}^{(L)} \cong 3.32$ and $\theta_{0.9-0.1}^{(S)} \cong 2.85$. In another words, the load carrying capacity for a longer fibre is indeed greater than that for a shorter one (cf. [37]).

Finally, in summary, we show that, in comparison to shorter carbon fibres at dynamically varying stress loadings, longer ones are more advantageous in competitiveness, though, during static stress loading, are less advantageous in strength. Interestingly, the analogous 'maximizing-competitive-advantage-while-minimizing-strength-to-failure' framework is characteristic of the high-energy systems such as missile windows [38] and explosives [39]. The final choice to select a

TABLE.

	$u_{0.1}$	$u_{0.5}$	$u_{0.9}$	$\theta_{0.9-0.1}$
Longer fibre	0.0585	6.764	123.17	3.323
Shorter fibre	0.0432	0.513	30.74	2.852

measure for the competitive advantage of carbon fibres can be made based on also the other requirements such as manufacturing cost and dynamic environment behaviour.

CONFLICTS OF INTEREST

Authors declare that there are no conflicts of interest between them.

ACKNOWLEDGMENTS

The present work was partially supported by the National Academy of Sciences of Ukraine (project No. 0121U109816).

REFERENCES

1. C. Perrow, *Normal Accidents: Living with High-Risk Technologies* (Princeton: Princeton University Press: 1999).
2. B. Rinner, *Telematik*, **2**: 6 (2002); ftp://www.iti.tu-graz.ac.at/pub/publications/rinner02b.pdf
3. M. Ferney, *Production Planning & Control*, **1**: 7 (2000); https://doi.org/10.1080/095372800232441
4. S. Y. Nof, G. Morel, L. Monostory, A. Molina, and F. Filip, *Annu. Rev. Control*, **30**: 55 (2006); https://doi.org/10.1016/j.arcontrol.2006.01.005
5. B. Jiang, L. Sun, D. R. Figueiredo, B. Ribeiro, and D. Towsley, *J. Stat. Phys. Theor. Exp.*, **2015**: 1 (2015); http://dx.doi.org/10.1088/1742-5468/2015/11/P11022
6. C. Mutua, *Int. J. Adv. Res. Manag. Soc. Sci.*, **8**: 23 (2019); http://garph.co.uk/IJARMSS/May2019/G-2538.pdf
7. A. L. Kuzemsky, *Statistical Mechanics and the Physics of Many-Particle Model Systems* (Singapore: World Scientific: 2017).
8. A. N. Gorban, *Entropy*, **16**: 2408 (2014); https://doi.org/10.3390/e16052408
9. V. I. Teslenko and O. L. Kapitanchuk, *Mod. Phys. Lett. B*, **32**: 1850022 (2018); https://doi.org/10.1142/S0217984918500227
10. O. L. Kapitanchuk and V. I. Teslenko, *Mol. Cryst. Liqu. Cryst.*, **670**: 119 (2018); https://doi.org/10.1080/15421406.2018.1542072
11. O. L. Kapitanchuk, O. M. Marchenko, and V. I. Teslenko, *Chem. Phys.*, **472**: 249 (2016); https://doi.org/10.1016/j.chemphys.2016.03.007
12. P. W. Anderson, *Phys. Rev.*, **109**: 1492 (1958); https://doi.org/10.1103/PhysRev.109.1492
13. V. Lubchenko and P. G. Wolynes, *Adv. Chem. Phys.*, **136**: 95 (2007); https://doi.org/10.1002/9780470175422
14. K. Kassner and R. Silbey, *J. Phys. Condens. Matter*, **1**: 4599 (1989); https://doi.org/10.1088/0953-8984/1/28/009
15. D. E. Bray, *Nondestructive Testing Techniques* (New York: John Wiley & Sons: 1992).
16. L. Cartz, *Nondestructive Testing* (Materials Park: ASM International: 1995).

17. R. C. Hibbeler, *Mechanics of Materials* (Upper Saddle River: Pearson Prentice Hall: 2014).
18. G. Vertesy, A. Gasparics, I. Szenthe, F. Gillemot, and I. Uytdenhouwen, *Materials*, **12**: 963 (2019); https://doi.org/10.3390/ma12060963
19. T. L. Anderson, *Fracture Mechanics—Fundamentals and Application* (Boca Raton: CRC Taylor & Francis: 2005).
20. *Polymer Testing* (Eds. W. Grellmann and S. Seidler) (Munich: Carl Hanser Verlag: 2013).
21. J. B. Watchman, W. R. Cannon, and M. J. Matthewson, *Mechanical Properties of Ceramics* (Hoboken: John Wiley & Sons: 2009).
22. R. Morrell, *Fractography of Brittle Materials* (Teddington: National Physical Laboratory: 1999).
23. S. van der Zwaag, *Self-Healing Materials: An Alternative Approach to 20 Centuries of Material Science* (Ed. S. van der Zwaag) (Dordrecht: Springer: 2007), p. 1.
24. R. Mikkilineni, *Designing a New Class of Distributed Systems* (Dordrecht: Springer: 2011).
25. A. L. Yarin, M. W. Lee, S. An, and S. S. Yoon, *Self-Healing Nanotextured Vascular Engineering Materials* (Cham: Springer Nature Switzerland AG: 2019).
26. *Progress in System Engineering. Advances in Intelligent Systems and Computing* (Eds. H. Selvaraj, D. Zydek, and G. Chmaj) (Cham: Springer International Publishing Switzerland: 2015).
27. S. G. Russell and P. Norvig, *Artificial Intelligence: A Modern Approach* (Edinburg: Pearson Education Limited: 2016).
28. K. S. Cheong, E. P. Busso, and A. Arsenlis, *Int. J. Plasticity*, **21**: 1797 (2005); https://doi.org/10.1016/j.ijplas.2004.11.001
29. F. Yang, *Mater. Sci. Eng. A*, **409**: 153 (2005); https://doi.org/10.1016/j.msea.2005.05.117
30. G. S. S. Gomes, N. B. Ludermir, and L. M. M. R. Lima, *Neural Comp. Appl.*, **20**: 417 (2011); https://doi.org/10.1007/s00521-010-0407-3
31. P. Peczak and M. J. Luton, *Phil. Mag. B*, **68**: 115 (1993); https://doi.org/10.1080/13642819308215285
32. H. Chang, J. Luo, P. V. Gulgunje, and S. Kumar, *Annu. Rev. Mater. Res.*, **47**: 331 (2017); https://doi.org/10.1146/annurev-matsci-120116-114326
33. M. Zou, W. Zhao et al., *Adv. Mater.*, **2018**: 1704419 (2018); https://doi.org/10.1002/adma.201704419
34. J. G. Lavin, *High-Performance Fibers* (Ed. J. W. S. Hearle) (Cambridge: Woodhead Publishing Ltd.: 2001), p. 156.
35. I. L. Kalnin, *Fracture of Composite Materials* (Eds. G. S. Sih and V. P. Tamuzs) (The Hague: Martinus Nijhoff Publishers: 1982), p. 465.
36. D. M. Bennett, *Characterizing The Fiber-Matrix Interphase Via Single Fiber Composite Tests* (Thesis of Disser. for Ph. D.) (Gainesville: University of Florida Press: 2007); http://etd.fcla.edu/UF/UFE0010097/bennett_d.pdf
37. Y.-T. Cho, T. Tohgo, and H. Ishii, *JSME Int. J. A*, **40**: 234 (1997); https://doi.org/10.1299/jsmea.40.234
38. C. A. Klein, *Opt. Eng.*, **37**: 2826 (1998); https://doi.org/10.1117/1.601820
39. P. Politzer, J. S. Murray, J. M. Seminario, P. Lane, M. E. Grice, and M. C. Concha, *J. Mol. Struct. (Theochem)*, **273**: 1 (2001); https://doi.org/10.1016/S0166-1280(01)00533-4